JOURNAL OF THERMOPHYSICS AND HEAT TRANSFER
Vol. 14, No. 3, July–September 2000

Effective Permeability for Natural Convection in a Layered Porous Annulus

C. C. Ngo* and F. C. Lai†
University of Oklahoma, Norman, Oklahoma 73019

The feasibility of using a lumped-system approach in the heat-transfer analysis of a layered porous annulus is numerically investigated. Numerical calculations have covered a wide range of parameters (i.e., $10 \le Ra_1 \le 500$, $0.01 \le K_1/K_2 \le 100$) for various sublayer thickness ratios ($\frac{5}{8} \le r_i/D \le \frac{11}{8}$). The results obtained are then presented in term of the effective Rayleigh number, which is defined based on the effective permeability. Three averaging techniques (i.e., arithmetic, harmonic, and volumetric) are used for the evaluation of the effective permeability. The results show that the lumped-system approach can provide a reasonably good prediction in heat transfer if an effective permeability is correctly chosen for the correlation.

Nomenclature

D = gap width, $r_2 - r_1$, m
g = acceleration from gravity, m/s^2
h = average heat-transfer coefficient, W/m$^2 \cdot$ K
K = permeability, m^2
$\bar{K}_A$ = effective permeability based on arithmetic average, m^2
$\bar{K}_H$ = effective permeability based on harmonic average, m^2
$\bar{K}_V$ = effective permeability based on volumetric average, m^2
k = effective thermal conductivity of porous medium, W/m $\cdot$ K
Nu = average Nusselt number, hD/k
$\overline{Nu}$ = normalized Nusselt number, Nu/Nu_{cond}
Nu_{cond} = conduction Nusselt number
p = pressure, Pa
R = dimensionless radial distance, r/D
Ra_A = Rayleigh number based on the arithmetic average permeability, $\bar{K}_A g\beta(T_h - T_c)D/\alpha_1\nu$
Ra_H = Rayleigh number based on the harmonic average permeability, $\bar{K}_H g\beta(T_h - T_c)D/\alpha_1\nu$
Ra_i = sublayer Rayleigh number, $K_i g\beta(T_h - T_c)D/\alpha_i\nu$
Ra_V = Rayleigh number based on the volumetric average permeability, $K_V g\beta(T_h - T_c)D/\alpha_1\nu$
Ra_1 = Rayleigh number based on the first sublayer properties, $K_1 g\beta(T_h - T_c)D/\alpha_1\nu$
r = radial distance, m
r_i = radial location of the interface, m
T = temperature, K
T_m = mean temperature, $(T_h + T_c)/2$
U = dimensionless velocity in the radial direction, $U = 1/R(\partial\Psi/\partial\theta)$
u = Darcy velocity in the radial direction, $u = \alpha U/D$
V = dimensionless velocity in the angular direction, $V = -\partial\Psi/\partial R$
v = Darcy velocity in the angular direction, $v = \alpha V/D$
α = thermal diffusivity of porous medium, $k/(\rho c_p)_f$, m^2/s
β = coefficient of thermal expansion, $(-1/\rho)(\partial\rho/\partial T)_{p,}$, K^{-1}
Θ = dimensionless temperature $(T - T_m)/(T_h - T_c)$
θ = angular coordinate
μ = dynamic viscosity, kg/m $\cdot$ s
ν = kinematic viscosity, m^2/s
ρ = density of fluid, kg/m^3
Ψ = dimensionless stream function

Presented as Paper 98-2676 at the AIAA/ASME 7th Joint Thermophysics and Heat Transfer Conference, Albuquerque, NM, 15–18 June 1998; received 11 August 1999; revision received 29 January 2000; accepted for publication 4 February 2000.

*Graduate Research Assistant, School of Aerospace and Mechanical Engineering. Student Member AIAA.
†Associate Professor, School of Aerospace and Mechanical Engineering. Senior Member AIAA.

Introduction

OVER the years, heat transfer in saturated porous media has received considerable attention because of its importance in many engineering applications. Although layered porous media are frequently encountered, they have received rather little attention as compared with homogeneous porous media. In addition, for the literature available in layered porous media[1–10] (a more comprehensive review of the subject is also available in Ref. 11) most of them dealt with the onset of natural convection and the characterization of the flow and temperature fields involved. Very few provide correlation for engineering applications. As a result, in many applications involving layered porous media a simple lumped-system approach is employed to expedite the heat-transfer calculation, instead of a detailed analysis of energy transfer in each sublayer. Clearly, the feasibility of a lumped-system approach is largely dependent on a successful characterization of the average properties of the system. Among the thermophysical properties involved, permeability is perhaps the most important one to be characterized because of its direct connection to the strength of convective flow. In this study an attempt has been made to characterize the effective permeability of a layered porous annulus subject to differential heating from the two bounding walls. Based on the results obtained, the feasibility of a lumped-system approach is evaluated. To this end, a detailed numerical analysis is performed over a wide range of parameters (i.e., $10 \le Ra_1 \le 500$ and $10^{-2} \le K_1/K_2 \le 10^2$) for various sublayer thickness ratios ($\frac{5}{8} \le r_i/D \le \frac{11}{8}$).

Formulation and Numerical Method

The geometry considered is a porous annulus comprising two sublayers (Fig. 1). While the outer wall is cooled at a constant temperature T_c, the inner wall is maintained at $T_h (T_h > T_c)$. The two sublayers that have a distinct permeability are assumed to be saturated with the same fluid. The governing equations based on Darcy's law are given by[9,10]

$$\frac{\partial u_i}{\partial r} + \frac{u_i}{r} + \frac{1}{r}\frac{\partial v_i}{\partial \theta} = 0 \tag{1}$$

$$u_i = -\frac{K_i}{\mu}\left(\frac{\partial p_i}{\partial r} + \rho g \sin\theta\right) \tag{2}$$

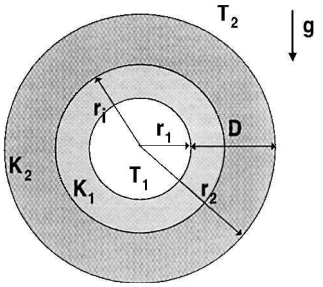

Fig. 1 Layered porous annulus subject to differential heating from two bounding walls.

$$v_i = -\frac{K_i}{\mu}\left(\frac{1}{r}\frac{\partial p_i}{\partial \theta} + \rho g \cos\theta\right) \tag{3}$$

$$u_i\frac{\partial T_i}{\partial r} + \frac{v_i}{r}\frac{\partial T_i}{\partial \theta} = \alpha_i\left(\frac{1}{r}\frac{\partial}{\partial r}\left(r\frac{\partial T_i}{\partial r}\right) + \frac{1}{r^2}\frac{\partial^2 T_i}{\partial \theta^2}\right) \tag{4}$$

where the subscript $i(=1, 2)$ denotes the inner and outer sublayers, respectively. The corresponding boundary conditions are the following.

On the inner wall:

$$T_1 = T_h, \qquad u_1 = 0 \tag{5a}$$

On the outer wall:

$$T_2 = T_c, \qquad u_2 = 0 \tag{5b}$$

At the interface the appropriate conditions are the continuity of pressure, temperature, radial flow, and heat flux:

$$p_1 = p_2 \tag{6a}$$

$$T_1 = T_2 \tag{6b}$$

$$u_1 = u_2 \tag{6c}$$

$$k_1\frac{\partial T_1}{\partial r} = k_2\frac{\partial T_2}{\partial r} \tag{6d}$$

The justification of these boundary conditions has been given by McKibbin and O'Sullivan,[2] as well as by Rana et al.[4]

After invoking Boussinesq approximation, the dimensionless governing equations are given by

$$\frac{\partial V_i}{\partial R} + \frac{V_i}{R} - \frac{1}{R}\frac{\partial U_i}{\partial \theta} = Ra_i\left(\cos\theta\frac{\partial \Theta_i}{\partial R} - \frac{\sin\theta}{R}\frac{\partial \Theta_i}{\partial \theta}\right) \tag{7}$$

$$U_i = \frac{\partial \Theta_i}{\partial R} + \frac{V_i}{R}\frac{\partial \Theta_i}{\partial \theta} = \frac{1}{R}\frac{\partial}{\partial R}\left(R\frac{\partial \Theta_i}{\partial R}\right) + \frac{1}{R^2}\frac{\partial^2 \Theta_i}{\partial \theta^2} \tag{8}$$

To solve the preceding two equations simultaneously, a coordinate transformation [Eq. (9)], which converts the computation domain onto a rectangular geometry, has been used to facilitate calculations:

$$x = \frac{\ell n R - \ell n R_1}{\ell n R_2 - \ell n R_1} - \frac{1}{2}, \qquad y = \frac{\theta - \theta_i}{\theta_o - \theta_i} - \frac{1}{2} \tag{9}$$

In the preceding expressions, R_1 and R_2 are the dimensionless inner radius and outer radius of the annulus. Also, $\theta_i(=0)$ and $\theta_o(=2\pi)$ represent the angular spans of the annulus.

This numerical scheme was previously employed by Pop and Lai[12] to simulate the natural convection in a truncated circular sector of porous medium. Although other transformations are possible, this approach is chosen because of its readiness for use with a minimum modification.

Thus, the governing equations in terms of stream function are transformed to

$$x_o^2\frac{\partial^2 \Psi_i}{\partial x^2} + y_o^2\frac{\partial^2 \Psi_i}{\partial y^2} = Ra_i(R_1R_2)^{\frac{1}{2}}\left(\frac{R_2}{R_1}\right)^x \times\left(x_o\frac{\partial \Theta_i}{\partial x}\cos\left(\frac{y}{y_o} + \theta_m\right) - y_o\frac{\partial \Theta_i}{\partial y}\sin\left(\frac{y}{y_o} + \theta_m\right)\right) \tag{10}$$

$$x_oy_o\left(\frac{\partial \Psi_i}{\partial y}\frac{\partial \Theta_i}{\partial x} - \frac{\partial \Psi_i}{\partial x}\frac{\partial \Theta_i}{\partial y}\right) = x_o^2\frac{\partial^2 \Theta_i}{\partial x^2} + y_o^2\frac{\partial^2 \Theta_i}{\partial y^2} \tag{11}$$

where

$$x_o = 1/[\ell n(R_2/R_1)], \qquad y_o = 1/(\theta_o - \theta_i) = 1/2\pi$$

$$\theta_m = (\theta_o + \theta_i)/2$$

Similarly, the boundary conditions are then expressed as follows. On the inner wall:

$$\Theta_1 = \tfrac{1}{2}, \qquad \Psi_1 = 0 \tag{12a}$$

On the outer wall:

$$\Theta_2 = -\tfrac{1}{2}, \qquad \Psi_2 = 0 \tag{12b}$$

whereas the interface conditions are given by

$$\frac{\partial \Psi_1}{\partial x} = \frac{K_1}{K_2}\frac{\alpha_2}{\alpha_1}\frac{\partial \Psi_2}{\partial x} \tag{13a}$$

$$\Theta_1 = \Theta_2 \tag{13b}$$

$$\frac{\partial \Psi_1}{\partial y} = \frac{\alpha_2}{\alpha_1}\frac{\partial \Psi_2}{\partial y} \tag{13c}$$

$$\frac{\partial \Theta_1}{\partial x} = \frac{\alpha_2}{\alpha_1}\frac{\partial \Theta_2}{\partial x} \tag{13d}$$

Because both sublayers are saturated with the same fluid, it is important to note that $\alpha_1/\alpha_2 = k_1/k_2$. The interface conditions have been implemented in the same way as described by Rana et al.[4] by using the imaginary nodal points.

The governing equations and boundary conditions are solved using a finite difference method, which has been successfully employed by the author.[9,10,12] In view of the complexity involved, the present study is limited to the case of $r_1/D = \frac{1}{2}$ and $r_2/D = \frac{3}{2}$. In addition, the diffusivity ratio α_1/α_2 is set to unity, assuming that the porous layers are made from the same material. A uniform grid, 51×121, has been used for most calculations in the present study, whereas finer grids (61×121, 81×121, and 101×121) are necessary for a few cases at $K_1/K_2 = 0.01$ to obtain converged solutions. Once solutions converged using the preceding specified grids, further grid refinement does not produce any significant improvement in the calculated Nusselt numbers. For example, the improvement in the predicted Nusselt number at $Ra_1 = 500$ is less than 2% when the grid is refined from 51×121 to 101×121. As an additional check on the accuracy of the computational results, an overall energy balance has been performed after each calculation. For the present study the energy balance for most calculations is satisfied within 2%. Only a few cases at $K_1/K_2 = 0.01$ are slightly greater than 2%. To validate the numerical code, the solutions thus obtained have been compared with those reported in the literature for the case of a homogeneous annulus by setting K_1/K_2 and $k_1/k_2(=\alpha_1/\alpha_2)$ to unity. The agreement is very good, as shown in Fig. 2 (Refs. 8 and 13–15).

Results and Discussion

For a layered porous annulus the flow and temperature profiles are very different from those of a homogeneous one caused by the step change in permeabilities. In addition, the location of the layer interface has a significant impact on the flow and temperature fields as will be discussed in the following sections.

For a homogeneous porous annulus the buoyancy-induced flow has a pattern of two primary cells (Fig. 3). Heated fluid rises to

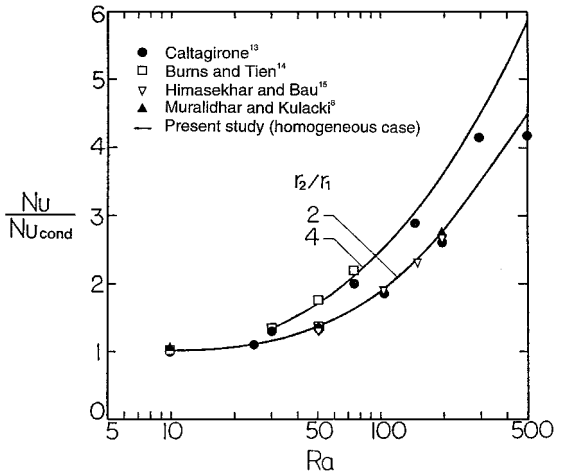

Fig. 2 Comparison of numerical results for natural convection in a homogeneous porous annulus.

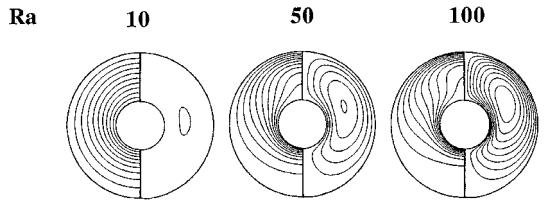

Fig. 3 Flow and temperature fields in a homogeneous porous annulus.

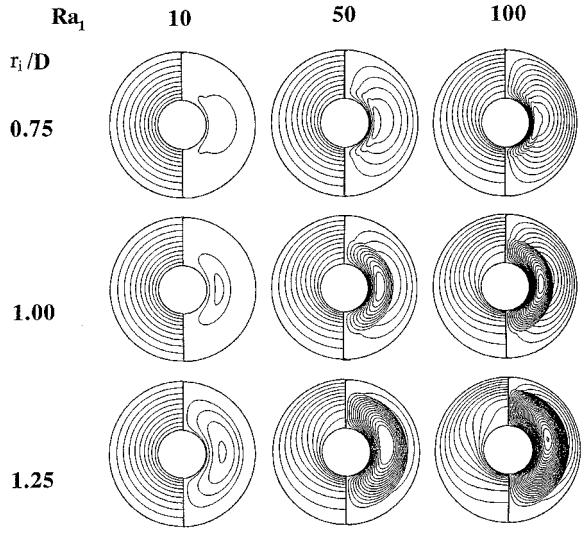

Fig. 4 Flow and temperature fields for a layered porous annulus with $K_1/K_2 = 10$ ($\Delta\Psi = 0.2$ and $\Delta\Theta = 0.1$).

the top along the inner cylinder and descends to the bottom of the annulus when cooled. Corresponding to this flow motion, a thermal plume is observed rising from the inner cylinder. Because of symmetry, isotherms are only shown on the left-hand side of the annulus, and streamlines are on the right-hand side. For a layered annulus the flow and temperature profiles are very different from those of a homogeneous one because of the step change in permeabilities (Figs. 4–7).

For $K_1/K_2 = 10$ convection was initiated in the inner sublayer at a small Rayleigh number. With an increase in the base Rayleigh number Ra_1, the progressive penetration of convective flow to the less permeable (outer) sublayer (Fig. 4) is clearly observed. However, for $K_1/K_2 = 100$ the outer sublayer behaves like an impermeable wall, and convection is completely confined to the inner sublayer. The flowfield in the inner sublayer looks almost identical to that of a homogeneous annulus with a reduced radius ratio of r_i/r_1 (Fig. 5).

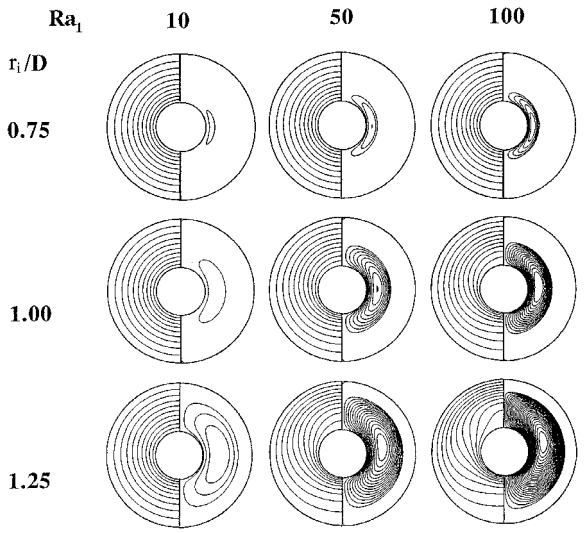

Fig. 5 Flow and temperature fields for a layered porous annulus with $K_1/K_2 = 100$ ($\Delta\Psi = 0.2$ and $\Delta\Theta = 0.1$).

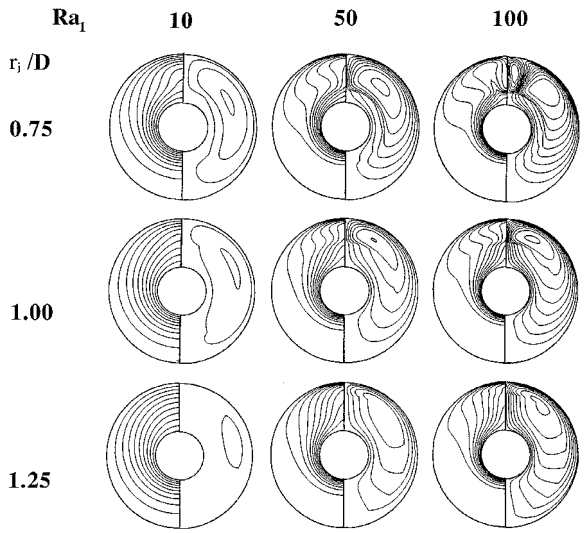

Fig. 6 Flow and temperature fields for a layered porous annulus with $K_1/K_2 = 0.1$ ($\Delta\Psi = 2$ and $\Delta\Theta = 0.1$).

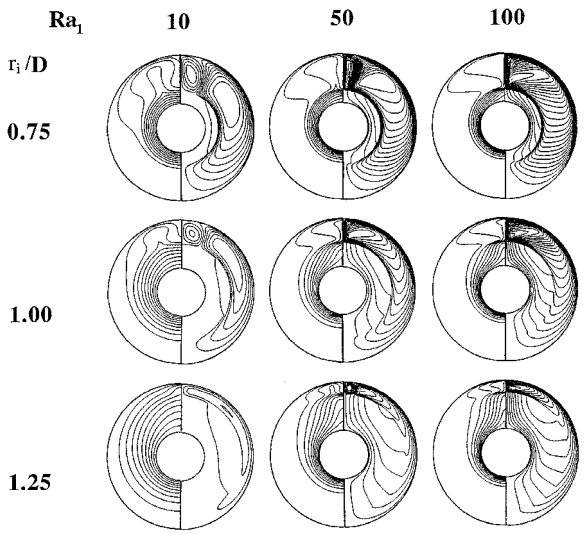

Fig. 7 Flow and temperature fields for a layered porous annulus with $K_1/K_2 = 0.01$ ($\Delta\Psi = 2$ and $\Delta\Theta = 0.1$).

As a result of flow confinement, heat transfer by convection is dominant in the inner sublayer and conduction in the outer sublayer. The difference in the heat-transfer mode involved in each sublayer can be clearly observed from the isotherms shown in Fig. 5. For $K_1/K_2 < 1$ convection is first initiated from the outer (more permeable) layer. With an increase in the Rayleigh number, convection also prevails in the inner sublayer (Figs. 6 and 7). It is interesting to observe the presence of secondary convective cells in the outer sublayer.

For a fixed Rayleigh number, the observation is made that the strength of convective cell increases with the sublayer thickness ratio r_i/D for $K_1/K_2 > 1$ (Figs. 4 and 5) and decreases for $K_1/K_2 < 1$ (Figs. 6 and 7). For $K_1/K_2 < 1$ a smaller thickness ratio leads to a suppression of convection in the inner layer and thus a higher interface temperature between two sublayers (Figs. 6 and 7). This consequently initiates a stronger convective cell in the outer layer. With an increase in the thickness ratio, the temperature gradient across the inner layer decreases, and the strength of the convective cell in the outer layer also reduces accordingly. Because of the permeability contrast, the result of this change is a slight increase in the strength of the convective cell in the inner layer, but a significant reduction in the outer layer. For $K_1/K_2 > 1$ the situation is just reversed.

For $K_1/K_2 > 1$ the contribution to total heat transfer by conduction from the less permeable (outer) layer increases as the thickness ratio increases, which is evident from the isotherms displayed in Figs. 6 and 7. On the other hand, for $K_1/K_2 < 1$ the contribution by convection from the less permeable layer increases as the thickness ratio increases.

The preceding discussion can be best understood by visualizing the step change in the permeability being created by replacing the outer portion of an originally homogeneous annulus with a different material (i.e., K_1 is held constant). When this is done by introducing a less permeable material to the outer region (i.e., $K_1/K_2 > 1$), the added flow resistance in the outer layer inhibits the penetration of the convective flow such that the recirculating cell is primarily confined to the inner layer. The outer sublayer in this case acts like a convection suppressor (Figs. 4 and 5). If a more permeable material is emplaced instead (i.e., $K_1/K_2 < 1$), the convective cell becomes notably strong when compared with that of a uniform case (Figs. 6 and 7). Because less flow resistance is encountered in the outer layer, the buoyancy-induced flow is initiated at a smaller Rayleigh number. The outer sublayer thus acts like a convection promoter. Because of the difference in the role played by the outer sublayer, the heat-transfer modes in these two cases are also distinct. For a layered annulus with $K_1/K_2 > 1$, heat transfer is mainly by conduction at a small Rayleigh number, which is evident from the corresponding isotherms shown in Figs. 4 and 5. As the Rayleigh number increases, it changes gradually from conduction to weak convection. On the other hand, heat transfer is always by convection for a layered annulus with $K_1/K_2 < 1$ (Figs. 6 and 7).

For the present study the total heat transfer from the annulus is of the greatest interest and can be expressed in terms of the Nusselt number

$$Nu = -\frac{1}{R_1 \ln(R_2/R_1)} \int_{-\frac{1}{2}}^{\frac{1}{2}} \left.\frac{\partial \theta}{\partial X}\right|_{x=-\frac{1}{2}} dy \tag{14}$$

Physically, this value represents the total heat fluxes from the inner cylinder. However, heat-transfer results for the problem under consideration are most informative if the Nusselt number thus obtained is normalized by its conduction value. In this way the normalized Nusselt number also represents the relative importance of convection to conduction. The conduction Nusselt number can be evaluated as

$$Nu_{\text{cond}} = 1/[R_1 \ln(R_2/R_1)] \tag{15}$$

and the normalized Nusselt number is thus given by

$$\overline{Nu} = \frac{Nu}{Nu_{\text{cond}}} = \int_{-\frac{1}{2}}^{\frac{1}{2}} \left.\frac{\partial \Theta}{\partial x}\right|_{x=-\frac{1}{2}} dy \tag{16}$$

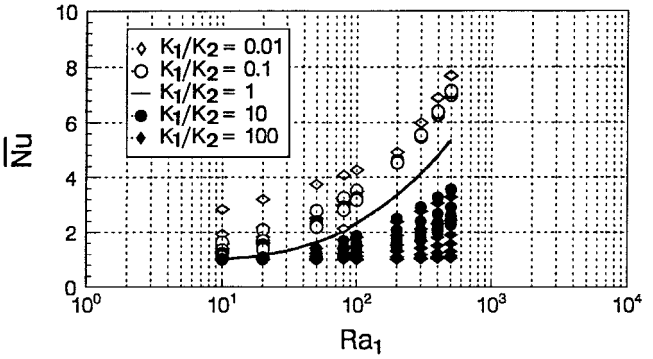

Fig. 8 Heat-transfer results for natural convection from a layered porous annulus.

The normalized Nusselt numbers obtained for the present study are shown in Fig. 8. The observation is made that the Nusselt number for a layered annulus of $K_1/K_2 < 1$ is always greater than that of a homogeneous annulus. But the Nusselt number for a layered annulus of $K_1/K_2 > 1$, on the other hand, is constantly smaller than that of a homogeneous one. The correlation for natural convection in a homogeneous annulus obtained from the present study is given by

$$\overline{Nu} = 0.238 Ra^{\frac{1}{2}} \tag{17}$$

which compares very well with the correlation proposed by Bejan[16]

$$\overline{Nu} = 0.223 Ra^{\frac{1}{2}} \tag{18}$$

based on the data reported by Caltagirone.[13]

As mentioned earlier, it is a common practice to use a lumped-system analysis for problems involving a layered system. Here, three averaging schemes are examined for their appropriateness in defining the effective permeability of a layered porous annulus. The first is based on the arithmetic average, the second is based on the harmonic average and the last is based on the volumetric average. The expressions for these averaging techniques are given next:

$$\bar{K}_A = \frac{r_i}{D} K_1 + \left(1 - \frac{r_i}{D}\right) K_2 \tag{19a}$$

$$\frac{1}{\bar{K}_H} = \frac{r_i/D}{K_1} + \frac{(1 - r_i/D)}{K_2} \tag{19b}$$

$$\bar{K}_V = \frac{\left(r_i^2 - r_1^2\right)}{\left(r_2^2 - r_1^2\right)} K_1 + \frac{\left(r_2^2 - r_i^2\right)}{\left(r_2^2 - r_1^2\right)} K_2 \tag{19c}$$

The heat-transfer results for natural convection in a layered porous annulus are redrawn in Fig. 9 as a function of the effective Rayleigh number, which is defined based on the effective permeability given in Eq. (19). Also shown in these figures is the numerical result obtained from the correlation [i.e., Eq. (17)]. From Fig. 9 the observation is clearly made that arithmetic and volumetric averaging schemes tend to underestimate the total heat transfer when compared with that predicted by the correlation. Despite some scattering, the effective permeability based on the harmonic average actually provides a better prediction in heat transfer. If it were used for engineering applications, the maximum error is estimated to be within 30% of that predicted by the correlation [Eq. (17)].

From a recent study[17] on natural convection in a layered square cavity, it is reported that the effective permeability of a layered system depends on the relative direction of the heat flow to the layer interface. In addition, the arithmetic average works better with a system in which heat flows in parallel to the layer interface, and the harmonic scheme is the best for a system in which heat flows perpendicularly to the layer interface. For a layered annulus subject to differential heating from two bounding walls, the relative direction of heat flow to the layer interface is rather complicated. Although heat flows nearly parallel to the interface in the lower half of the annulus, it is almost perpendicular to the interface in the upper half of

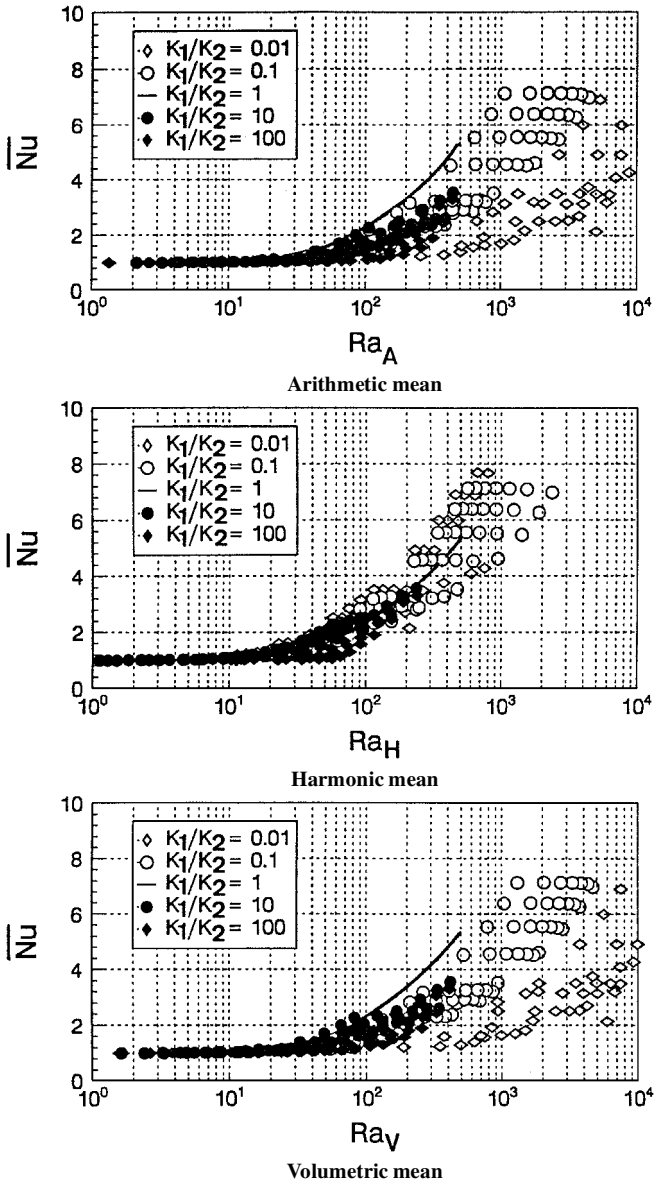

Fig. 9 Heat-transfer results based on the effective permeability model.

the annulus. As a result, the characterization of effective permeability for a layered annulus is not as straightforward as that for a layered square cavity. Although some success in using the harmonic scheme has been observed in the present study, the data in the present study are scattered slightly wider than those of layered square cavities,[17] which seems to imply that the present analysis needs to be further refined. To combine both arithmetic and harmonic schemes with a weighting parameter has been attempted. The results, however, were not satisfactory.

Conclusions

Heat transfer across a layered porous annulus has been numerically examined. Whereas the present study has explored a fundamental heat-transfer problem in a layered porous annulus, the study has primarily focused on the feasibility of using a lumped-system approach in the heat-transfer analysis. Based on the results obtained, one can conclude that a lumped-system approach is applicable for heat-transfer analysis in a layered system as long as the effective permeability is correctly chosen for the correlation. For the present study the harmonic averaging scheme provides the best results. The error that can result from using this approach is estimated to be within 30% of that predicted by the correlation. Effects of other nonuniform properties on the applicability of a lumped-system analysis to a layered system await further investigation.

References

[1]McKibbin, R., and O'Sullivan, M. J., "Onset of Convection in a Layered Porous Medium Heated from Below," *Journal of Fluid Mechanics*, Vol. 96, No. 2, 1980, pp. 375–393.

[2]McKibbin, R., and O'Sullivan, M. J., "Heat Transfer in a Layered Porous Medium Heated from Below," *Journal of Fluid Mechanics*, Vol. 111, Oct. 1981, pp. 141–173.

[3]McKibbin, R., and Tyvand, P. A., "Anisotropic Modelling of Thermal Convection in Multilayered Porous Media," *Journal of Fluid Mechanics*, Vol. 118, May 1982, pp. 315–339.

[4]Rana, R., Horne, R. N., and Cheng, P., "Natural Convection in a Multi-Layered Geothermal Reservoir," *Journal of Heat Transfer*, Vol. 101, No. 3, 1979, pp. 411–416.

[5]Poulikakos, D., and Bejan, A., "Natural Convection in Vertically and Horizontally Layered Porous Media Heated from the Side," *International Journal of Heat and Mass Transfer*, Vol. 26, No. 12, 1983, pp. 1805–1814.

[6]Lai, F. C., and Kulacki, F. A., "Natural Convection in Layered Porous Media Partially Heated from Below," *Heat Transfer in Geophysical and Geothermal System*, edited by K. Vafai, V. Prasad, and I. Catton, ASME HTD-Vol. 76, American Society of Mechanical Engineers, New York, 1987, pp. 27–36.

[7]Lai, F. C., and Kulacki, F. A., "Natural Convection Across a Vertical Layered Porous Cavity," *International Journal of Heat and Mass Transfer*, Vol. 31, No. 6, 1988, pp. 1247–1260.

[8]Muralidhar, K., Baunchalk, R. A., and Kulacki, F. A., "Natural Convection in a Horizontal Porous Annulus with a Step Distribution in Permeability," *Journal of Heat Transfer*, Vol. 108, No. 4, 1986, pp. 889–893.

[9]Pan, C. P., and Lai, F. C, "Natural Convection in Horizontal Layered Porous Annuli," *Journal of Thermophysics and Heat Transfer*, Vol. 9, No. 4, 1995, pp. 792–795.

[10]Pan, C. P., and Lai, F. C., "Reexamination of Natural Convection in a Horizontal Layered Porous Annulus," *Journal of Heat Transfer*, Vol. 118, No. 4, 1996, pp. 990–992.

[11]Nield, D. A., and Bejan, A., *Convection in Porous Media*, 2nd ed., Springer-Verlag, New York, 1999, pp. 223–230.

[12]Pop, I., and Lai, F. C., "Natural Convection in a Truncated Circular Sector of Porous Medium," *International Communications in Heat and Mass Transfer*, Vol. 17, No. 6, 1990, pp. 801–811.

[13]Caltagirone, J. P., "Thermoconvective Instabilities in a Porous Medium Bounded by Two Concentric Horizontal Cylinders," *Journal of Fluid Mechanics*, Vol. 76, No. 2, 1976, pp. 337–362.

[14]Burns, P. J., and Tien, C. L., "Natural Convection in Porous Media Bounded by Concentric Spheres and Horizontal Cylinders," *International Journal of Heat and Mass Transfer*, Vol. 22, No. 6, 1979, pp. 929–939.

[15]Himasekhar, K., and Bau, H. H., "Large Rayleigh Number Convection in a Horizontal, Eccentric Annulus Containing Saturated Porous Media," *International Journal of Heat and Mass Transfer*, Vol. 29, No. 5, 1986, pp. 703–712.

[16]Bejan, A., "Convective Heat Transfer in Porous Media," *Handbook of Single-Phase Convective Heat Transfer*, edited by S. Kakaç, R. K. Shah, and W. Aung, Wiley, New York, 1987, pp. 16–20.

[17]Leong, J. C., and Lai, F. C., "Effective Permeability of a Layered Porous System," *Proceedings of the 7th AIAA/ASME Joint Thermophysics and Heat Transfer Conference*, edited by B. F. Armaly, ASME HTD-Vol. 357-2, American Society of Mechanical Engineers, New York, 1998, pp. 203–211.